Accepted Manuscript

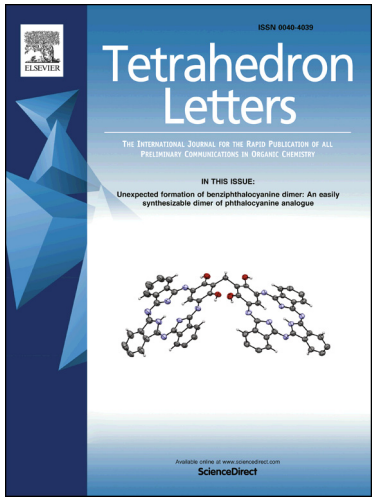

Naphthalene-derived Al^{3+}-selective fluorescent chemosensor based on PET and ESIPT in aqueous solution

Xiao-li Yue, Zhao-qing Wang, Chao-rui Li, Zheng-yin Yang

PII: S0040-4039(17)31336-9
DOI: https://doi.org/10.1016/j.tetlet.2017.10.044
Reference: TETL 49406

To appear in: *Tetrahedron Letters*

Received Date: 5 August 2017
Revised Date: 15 October 2017
Accepted Date: 17 October 2017

Please cite this article as: Yue, X-l., Wang, Z-q., Li, C-r., Yang, Z-y., Naphthalene-derived Al^{3+}-selective fluorescent chemosensor based on PET and ESIPT in aqueous solution, *Tetrahedron Letters* (2017), doi: https://doi.org/10.1016/j.tetlet.2017.10.044

This is a PDF file of an unedited manuscript that has been accepted for publication. As a service to our customers we are providing this early version of the manuscript. The manuscript will undergo copyediting, typesetting, and review of the resulting proof before it is published in its final form. Please note that during the production process errors may be discovered which could affect the content, and all legal disclaimers that apply to the journal pertain.

ACCEPTED MANUSCRIPT

Naphthalene-derived Al^{3+}-selective fluorescent chemosensor based on PET and ESIPT in aqueous solution

Xiao-li Yue, Zhao-qing Wang, Chao-rui Li, Zheng-yin Yang*

College of Chemistry and Chemical Engineering, State Key Laboratory of Applied Organic Chemistry, Lanzhou University, Lanzhou 730000, P.R. China

***Corresponding author. Tel: +86 931 8913515; Fax: +86 931 812582; e-mail: yangzy@lzu.edu.cn (Z.Y. Yang)*

ABSTRACT

A simple fluorescent chemosensor **HL** based on naphthalene with high selectivity and sensitivity towards Al^{3+} over other commonly coexisting metal cations in fully aqueous solution to enhance the potential applications of the fluorescent chemosensor was developed. **HL** exhibited a significant fluorescence enhancement at 475 nm in the presence of Al^{3+} over other competitive metal ions with a low detection limit of 0.43 μM due to the inhibition of the photo induced electron transfer (PET) and the excited-state intramolecular proton transfer (ESIPT). The 1∶1 binding stoichiometry between **HL** and Al^{3+} was corroborated by the Job plot and the ESI-MS spectrum. Importantly, the reversible recognition process of **HL** to Al^{3+} will make **HL** could be used circularly and repeatedly in practical applications by addition of Na_2EDTA. In

ACCEPTED MANUSCRIPT

addition, the binding behavior and sensing mechanism of **HL** to Al^{3+} were illustrated in detail by the ^1H NMR titration experiment.

KEYWORDS: Fluorescent chemosensor; Naphthalene; Photo-induced electron transfer; Excited-state intramolecular proton transfer.

1. Introduction

The design and synthesis of fluorescent chemosensors for Al^{3+} continues to be a significant research subject. On the one hand, Al^{3+} has its impact on the environment and human health. On the other hand, fluorescent techniques show simplicity, high selectivity and sensitivity, on-site and real time monitoring, as well as low detection limit [1-6] compared with traditional analytical methods for detecting Al^{3+} such as ion selective membrane, atomic absorption spectrometry, voltammetry, inductively coupled plasma mass spectrometry (ICP-MS), and liquid chromatography mass spectrometry [7]. As the most prevalent metallic element (8.3% by weight) and the third most abundant element (after oxygen and silicon) in the earth's crust [8-10], aluminum is widely used in modern society involving industrial fields and daily life. In industrial fields, aluminum is diffusely used in water treatment, paper industry, dye production, textile industry, cosmetic preparations, production of light alloy, as well as manufacturing of cars and computers [11-16]. Additionally, in daily life, aluminum is far and wide used in food additions, food packaging, aluminum-based pharmaceuticals, storage/cooking utensils, and electrical equipment [17-24]. However, aluminum in excessive amounts would lead to environmental contamination and be toxic to human health [25,26]. Particularly, excess aluminum in the human body

ACCEPTED MANUSCRIPT

interferes with the calcium metabolism, causing Osteomalacia, influences the ingestion of iron in blood, causing microcytic hypochromic anemia, and also decreases liver and kidney function. Moreover, excess accumulation of Al^{3+} leads to malfunction of the central nervous system, which cause human illnesses such as encephalopathy, myopathy, dementia, Guamanian amyotrophic lateral sclerosis, Parkinson's disease, and Alzheimer's disease [27-33]. Therefore, it's essential and crucial to design and synthesize some fluorescent chemosensors for detecting Al^{3+} in the environmental and biological systems.

The development of Al^{3+} fluorescent probe is rather slow compared with other common transition metal ions due to the lack of spectroscopic characteristics and poor coordination ability [34]. Recently, many various fluorescent chemosensors for detecting Al^{3+} have been reported. However, many of them have suffered from many drawbacks such as synthesis based on single mechanism causing poor selectivity and sensitivity [35], tedious synthetic route [36], poor water solubility [36], and fluorogenic response in organic solvents making them difficult for practical applications [17]. Thus, it's highly desirable to develop some fluorescent chemosensors based on multi-mechanism for the detection of Al^{3+} in aqueous solution. Owing to the short fluorescence life time [34], the low fluorescence quantum yield [34], and the ability to act both as a donor as well as an acceptor [37], Naphthalene and its derivatives have been chosen as ideal components of some fluorescent chemosensors.

Hence, taking these factors into account, we have designed and synthesized a

ACCEPTED MANUSCRIPT

simple fluorescent chemosensor **(HL)** based on PET (photo induced electron transfer) [34] and ESIPT (excited-state intramolecular proton transfer) [38] for the detection of Al^{3+} in aqueous media, which enhanced the practical application of the chemosensor. The structure of **HL** was validated by ^1H NMR spectrum and the ESI mass spectrum. The 1∶1 binding stoichiometry between **HL** and Al^{3+} was confirmed by the Job's plot titration curve and the mass spectrum data. In addition, the recognition process of **HL** towards Al^{3+} was chemically reversible in the presence of Na_2EDTA with a quite low detection limit (0.43 μM) of a micromolar concentration level.

2. Experimental section

2.1. Materials and instruments

The materials used for this study were obtained from commercial suppliers and used without further purification. ^1H NMR spectrum were measured on the JNM-ECS 400 MHz spectrometer. Chemical shifts are reported in ppm using TMS as an internal standard. ESI-MS were determined on a Bruker esquire 6000 spectrometer. UV–vis absorption spectrum were measured with a Shimadzu UV-240 spectrophotometer. Fluorescence spectrum were determined on a Hitachi RF-4500 spectrophotometer equipped with quartz cuvettes of 1 cm path length. The melting point was determined on a Beijing XT4-100x microscopic melting point apparatus.

2.2. Synthesis

The synthetic route of **HL** (2-hydroxy-1-naphthaldehyde-(4-pyridinecarboxylic)-hydrazone) was shown in Scheme 1.

ACCEPTED MANUSCRIPT

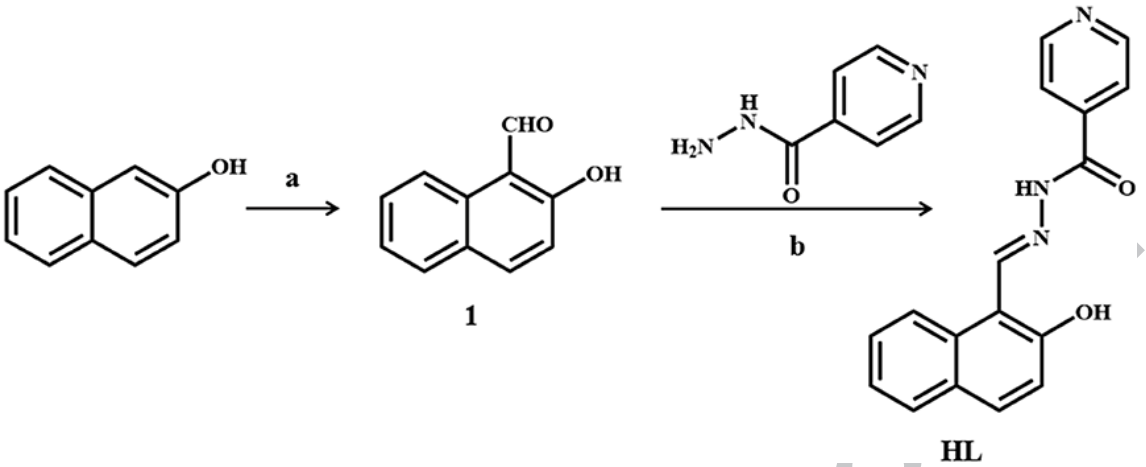

Scheme 1. The synthetic route of 2-hydroxy-1-naphthaldehyde-(4-pyridinecarboxylic) hydrazone (**HL**). Reagents and conditions: (a) HMTA, glacial acetic acid, reflux, 12 h; (b) EtOH, reflux, 10 h.

2.2.1. Synthesis of compound 1 (2-hydroxy-1-naphthaldehyde) [39]

A 10.5 g of 2-naphthol was added to a solution of a 12 g of Hexamethylenetetramine (HMTA) in 20 ml of acetic acid and then the reaction solution was stirred and heated for 1 h at 50-60 °C. After rising the temperature to 90 °C, H_2SO_4 (98%, 10 ml) was added dropwise to the above solution within 40 min. Upon adding completely, the temperature of the system was raised to 96 °C rapidly and then the reaction solution was refluxed for 10 h with stirring at 96 °C. After cooling to room temperature, 100 ml of ice-water mixture was added to precipitate the crude product. The crude product was collected and washed with cold water until the pH of the filtrate was neutral. The final product was recrystallized from ethanol and dried in vacuum at low temperature to obtain a yellow solid. Yield: 76%; mp: 79-80 °C. ^{1}H NMR (400 MHz, $CDCl_3$, TMS) (Figure S1): δ_H ppm 13.16 (s, 1H), 10.81 (s, 1H), 8.34 (d, 1H, J=8.8Hz), 7.98 (d, 1H, J=9.2Hz), 7.80 (d, 1H, J=8Hz), 7.62

ACCEPTED MANUSCRIPT

(t, 1H, J=8Hz), 7.44 (t, 1H, J=8Hz), 7.14 (d, 1H, J=9.2Hz).

2.2.2. Synthesis of 2-hydroxy-1-naphthaldehyde-(4-pyridinecarboxylic)hydrazone ***(HL)***

2-hydroxy-1-naphthaldehyde (0.69 g) and 4-pyridinecarboxylic hydrazide (0.55 g) were mixed in 20 ml ethanol and refluxed for 10 h under N_2. After cooling to room temperature, the precipitate was collected and washed 3 times with ethanol. Then the final product was recrystallized from ethanol and dried in vacuum to give a yellow solid. Yield: 79%; mp: 257 °C. ^{1}H NMR (400 MHz, DMSO-d_6, TMS) (Figure S2): δ_H ppm 12.49 (s, 1H), 12.37 (s, 1H), 9.44 (s, 1H), 8.80 (d, 1H, J=2.0Hz), 8.78 (d, 1H, J=2.0Hz), 8.28 (d, 1H, J=8.0Hz), 7.92 (d, 1H, J=8.0Hz), 7.88 (s, 1H), 7.86 (d, 1H, J=2.0Hz), 7.84 (d, 1H, J=2.0Hz), 7.58 (m, 1H), 7.38 (t, 1H, J=3.6Hz), 7.21 (d, 1H, J=8.0Hz). ^{13}C NMR (400 MHz, DMSO-d_6, TMS) (Figure S3): δ_C ppm 109.05, 119.36, 121.48, 121.97, 124.15, 128.39, 128.44, 129.53, 132.13, 133.66, 140.32, 148.51, 151.02, 158.72, 161.55 (C=O). ESI-MS (Figure S4) calculated for $[M+H]^+$ 292.3166, found 292.1458.

2.3. UV-vis and fluorescence spectrum measurements

Stock solutions of 5×10^{-3} M various metal ions and **HL** were prepared in ethanol. Additionally, the stock solution of 5×10^{-3} M Na_2EDTA was prepared in distilled water. All absorption and emission spectrum were performed in a quartz optical cell of 1 cm optical path length at room temperature. All fluorescence measurements were carried out upon excitation at 415 nm. Both excitation and emission slit widths were 3 nm.

3. Results and discussion

ACCEPTED MANUSCRIPT

To find out the effect of solvent in the fluorogenic response of **HL** towards Al^{3+}, we recorded the emission changes in different solvents (Figure S5). The fluorescence intensity of **HL** enhanced about 500-fold accompanied with the split of the fluorescence emission spectrum upon addition of Al^{3+} in methanol. The fluorescence intensity of **HL** strengthened approximately 400-fold and the phenomenon of the split still existed after the addition of Al^{3+} in ethanol. Furthermore, the fluorescence intensity of **HL** had different extent of enhancement and the phenomenon of the split still existed upon addition of Al^{3+} in other solvents. It was notable that the fluorescence intensity of **HL** enhanced about 550-fold and those bands just merge together due to increased inhomogeneity after the addition of Al^{3+} in water. Thus, further UV/vis and fluorescent studies were carried out in aqueous solution.

*3.1. UV-vis studies of **HL** towards Al^{3+}*

The UV/vis spectrum of **HL** towards various metal ions (Na^+, K^+, Ag^+, Ca^{2+}, Mg^{2+}, Ba^{2+}, Zn^{2+}, Cu^{2+}, Ni^{2+}, Cd^{2+}, Co^{2+}, Pb^{2+}, Mn^{2+}, Hg^{2+}, Cr^{3+}, Fe^{3+}, and Al^{3+}) was illustrated in Figure 1a. In the absence of Al^{3+}, **HL** exhibited characteristic absorption bands at 325 nm and 366 nm which should be assigned to $\Pi \rightarrow \Pi^*$ transitions of naphthalene ring [40-42]. Upon addition of Al^{3+} to **HL** solution, a new absorption peak at 432 nm appeared, while other metal ions showed no absorption peak at 432 nm under the identical conditions. Thus, **HL** could serve as a highly selective fluorescent probe for Al^{3+}.

The absorption titrations of **HL** towards Al^{3+} were carried out in aqueous solution (Figure 1b). Upon gradual addition of Al^{3+} to **HL** solution, the absorption

ACCEPTED MANUSCRIPT

bands at 325 nm and 366 nm gradually decreased while the new absorption band at 432 nm appeared with increasing intensity. Meanwhile, an isobestic point at 400 nm was observed. These results indicated that the formation of a new stable complex between **HL** and Al^{3+}. Moreover, the absorbance spectrum of **HL** exhibited no remarkable changes and the intensity of absorption remained constant more than *1 equiv. of* Al^{3+}, demonstrating the 1 □1 binding stoichiometry between **HL** and Al^{3+}.

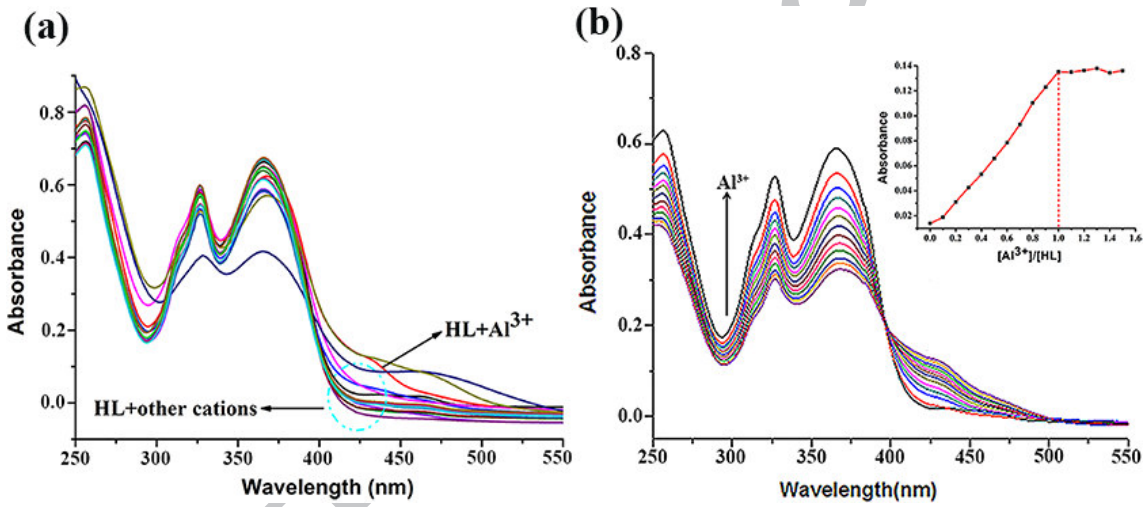

Figure 1. (a) UV-vis spectrum of **HL** before and after of *1 equiv. of* various metal cations in aqueous solution. (b) UV-vis absorption titration spectrum of **HL** (50 μM) with Al^{3+} (0-1.5 equiv.) in aqueous solution. Inset: Changes of absorbance intensity at 432 nm.

*3.2. Fluorescence studies of **HL** towards Al^{3+}*

As we all know, an ability of achieving highly selective fluorogenic response to the target analyte over other competitive species is an important characterization for a chemosensor. The optical properties of **HL** towards various metal ions were investigated by fluorescence emission spectrum in aqueous solution (Figure 2a). **HL** exhibited no fluorescence emission at 475 nm with a low fluorescence quantum yield

ACCEPTED MANUSCRIPT

(Φ=0.5%) upon excitation at 415 nm. Upon addition of *1 equiv. of* different metal ions (Na^+, K^+, Ag^+, Ca^{2+}, Mg^{2+}, Ba^{2+}, Zn^{2+}, Cu^{2+},Ni^{2+}, Cd^{2+}, Co^{2+}, Pb^{2+}, Mn^{2+}, Hg^{2+}, Cr^{3+}, Fe^{3+}, and Al^{3+}) to the system of **HL**, only Al^{3+} could cause a significant fluorescence enhancement at 475 nm with a high fluorescence quantum yield (Φ=26.4%), indicating that **HL** was a highly selective fluorescent probe for Al^{3+}.

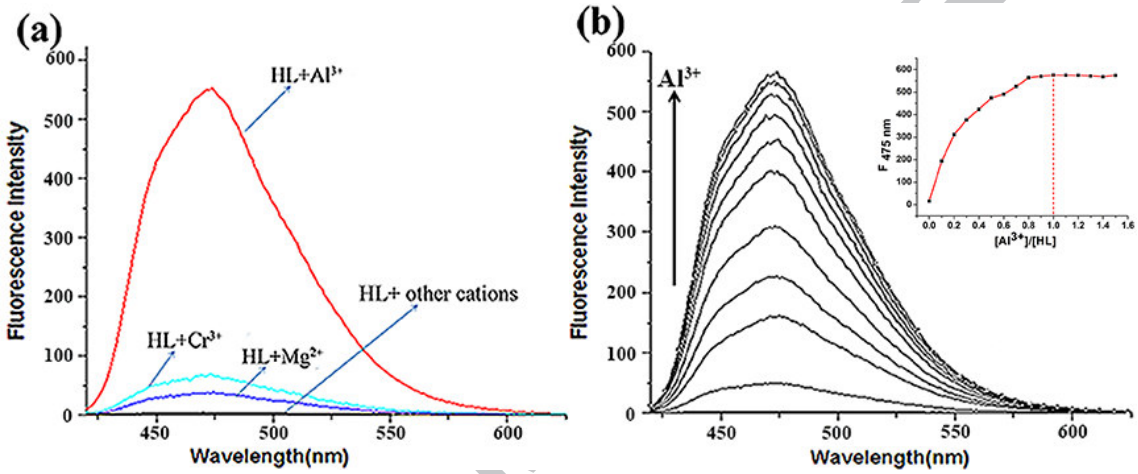

Figure 2. (a) The fluorescence emission spectrum of **HL** (50 μM) upon addition of *1 equiv. of* various metal ions (Na^+, K^+, Ag^+, Ca^{2+}, Mg^{2+}, Ba^{2+}, Zn^{2+}, Cu^{2+},Ni^{2+}, Cd^{2+}, Co^{2+}, Pb^{2+}, Mn^{2+}, Hg^{2+}, Cr^{3+}, Fe^{3+}, and Al^{3+}) in aqueous solution (λ_{ex}=415 nm; λ_{em}=475 nm). (b) The fluorescence emission spectrum of **HL** (50 μM) upon addition of Al^{3+} (0-1.5 equiv.) in aqueous solution (λ_{ex}=415 nm). Inset: Changes of fluorescence emission intensity at 475 nm.

The optical properties of **HL** towards Al^{3+} were also studied by fluorescence emission spectrum in aqueous solution (Figure 2b). The fluorescence intensity of **HL** gradually increased with the progressive addition of Al^{3+}. Furthermore, further increasing concentrations of Al^{3+} more than *1 equiv*, the fluorescence intensity of **HL** remained steady, which also suggested that 1 □1 binding model between **HL** and

ACCEPTED MANUSCRIPT

Al^{3+}.

3.3. Interference studies from other metal ions.

To evaluate the ability of resisting interference from other metal ions, we recorded the fluorescence emission changes of **HL** to Al^{3+} in the presence of other coexistent metal ions (Na^{+}, K^{+}, Ag^{+}, Ca^{2+}, Mg^{2+}, Ba^{2+}, Zn^{2+}, Cu^{2+},Ni^{2+}, Cd^{2+}, Co^{2+}, Pb^{2+}, Mn^{2+}, Hg^{2+}, Cr^{3+}, Fe^{3+}, and Al^{3+}) (Figure 3). It could be seen from Figure 3 that the competitive metal ions did not interfere with the detection of **HL** to Al^{3+} at the same conditions, which may due to the formation of a stable complex of **HL** with Al^{3+} compared with other competitive metal ions. The experimental results illustrated that **HL** still exhibited high selectivity for Al^{3+} over other competitive metal ions.

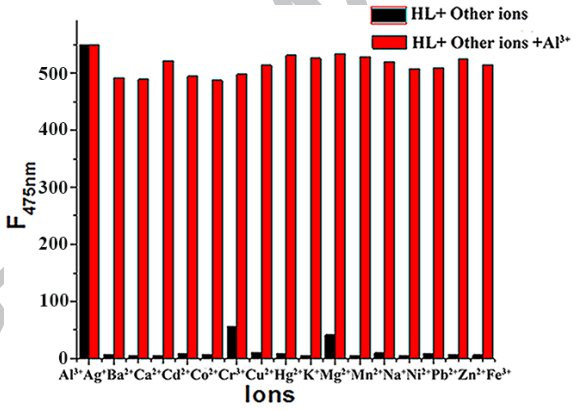

Figure 3. The fluorescence intensity at 475 nm of **HL** (50 μM) upon addition of various metal ions (black bars: **HL** with other metal ions; red bars: **HL** with other metal ions and Al^{3+}) in aqueous solution (λ_{ex}=415 nm).

*3.4. Reversible test of **HL** towards Al^{3+} by Na_2EDTA*

To estimate the practical applicability of **HL** as a selective fluorescent probe for Al^{3+}, the reversible experiment was carried out in aqueous solution (Figure 4). It was notable that **HL** showed significant fluorescence enhancement at 475 nm in the

ACCEPTED MANUSCRIPT

presence of *1 equiv. of* Al^{3+}, while the fluorescence intensity at 475 nm decreased remarkably upon addition of *1 equiv. of* Na_2EDTA due to the weak coordination ability of **HL** to Al^{3+} compared with that of Na_2EDTA to Al^{3+}. What's more, **HL** still exhibited a good fluorescence response towards Al^{3+} at least 5 cycles with small changes in fluorescence intensity at 475 nm when we added alternately Al^{3+} ion solution (5×10^{-3} M) and aqueous Na_2EDTA solution (5×10^{-3} M). The reversible test results demonstrated that the recognition process of **HL** to Al^{3+} was chemically reversible. Thus, **HL** could serve as a highly selective reversible fluorescent probe for detection and recognition of Al^{3+} in both biological assays and the environmental systems.

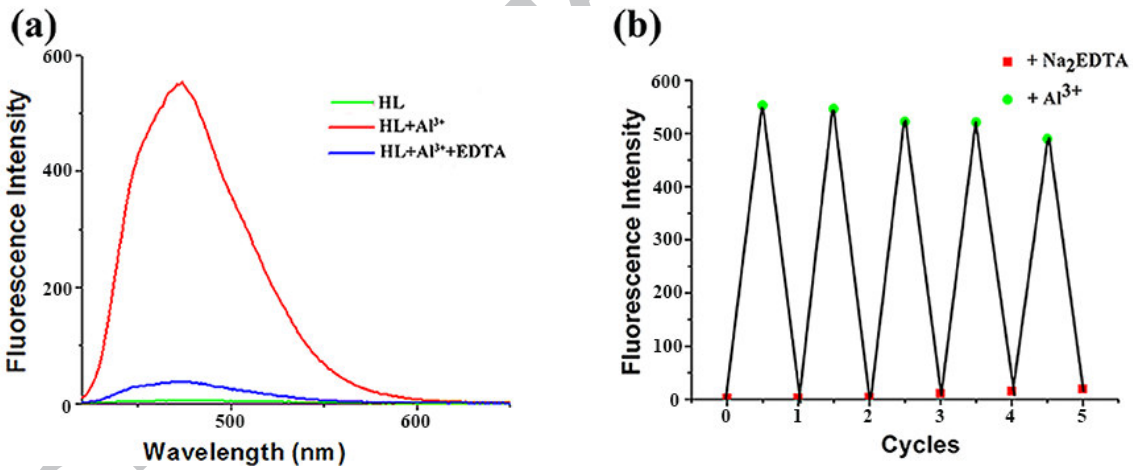

Figure 4. (a) The reversible experiment of **HL** towards Al^{3+} by adding Na_2EDTA in aqueous solution (λ_{ex}=415 nm). (b) The fluorogenic response of **HL** to Al^{3+} in the 5×10^{-3} M of Na_2EDTA over five complex/stripping cycles (λ_{ex}=415 nm).

3.5. Binding constant, stoichiometry and detection limit

The association constant (Ka) of **HL** to Al^{3+} was determined by the Benesi-Hildebrand equation: $\frac{1}{F-F_{min}} = \frac{1}{K(F_{max}-F_{min})[Al^{3+}]} + \frac{1}{F_{max}-F_{min}}$ where F is the fluorescence

ACCEPTED MANUSCRIPT

intensity at 475 nm at any given Al^{3+} concentration, F_{min} is the fluorescence intensity at 475 nm in the absence of Al^{3+}, and F_{max} is the maximal fluorescence intensity at 475 nm in the presence of Al^{3+} [43]. The Ka value was calculated to be 5.17×10^4 M^{-1} according to the plotting $1/ (F-F_{min})$ against $1/ [Al^{3+}]$ (Figure S6). The detection limit (LOD) of **HL** to Al^{3+} was calculated to be 0.43 μM according to the equation: $DL=3\sigma/K$ where σ is the standard deviation of the blank solution and K is the slope of the calibration curve (Figure S8) from the fluorescence titration experiments (Figure S7) [43]. Additionally, the binding stoichiometry of **HL** to Al^{3+} was determined by the Job's method on the basis of fluorescence emission spectrum. It could be seen from Figure 5 that the fluorescence intensity at 475 nm exhibited a maximum when the molar fraction of **HL** was 0.5 demonstrating a possible 1 □1 binding stoichiometry between **HL** and Al^{3+}. To better understand the coordination mode of **HL** to Al^{3+}, the ESI mass spectrum of **HL** in the presence of Al^{3+} was carried out (Figure S9). The m/z peak for **HL** in the presence of Al^{3+} at 380.1554 appeared, which was assigned to $[\mathbf{HL}+Al^{3+}+H_2O+CH_3CH_2OH-2H^+]^+$. The mass spectrum analysis gave another solid evidence for the 1 □1 binding model between **HL** and Al^{3+}.

ACCEPTED MANUSCRIPT

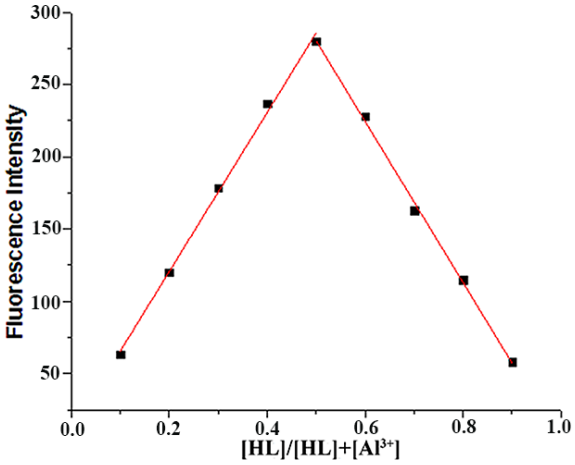

Figure 5. Job's plot for determining the binding stoichiometry of **HL** and Al^{3+} in aqueous solution. The total concentration of **HL** and Al^{3+} was kept 100 μM (λ_{ex}=415 nm).

*3.6. Proposed sensing mechanism of **HL** towards Al^{3+}*

It is well known that the proton chemical shift of coordination atom of ligands will change when metal ion coordinates with ligands. To better understand the binding behavior and sensing mechanism of **HL** to Al^{3+}, the ^{1}H NMR titration experiment of **HL** was performed in the presence of *1 equiv. of* Al^{3+} (Figure 6). It was prominent that the proton signals of H_a (-OH) and H_b (-NH) disappeared upon addition of Al^{3+}. Moreover, the proton signal of H_c (-CH=N) shifted downfield from δ 9.44 ppm to δ

ACCEPTED MANUSCRIPT

ACCEPTED MANUSCRIPT

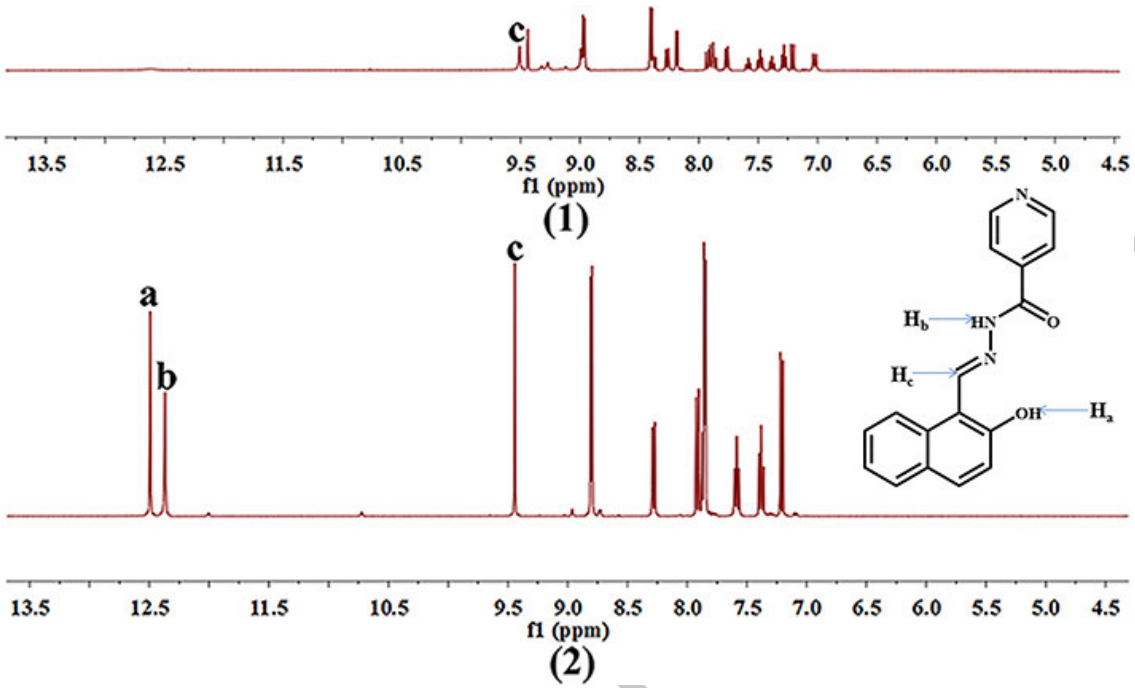

Figure 6. The ^{1}H NMR spectrum of **HL** with and without Al^{3+} in DMSO-d_6 (400 MHz): **HL** (2); **HL** with *1 equiv of* Al^{3+} (1). Inset: The image of the structure of **HL**.

9.51 ppm in the presence of Al^{3+}. The above findings demonstrated that the probable binding mode (Scheme 2) was that the oxygen atoms of the hydroxyl group and the carbonyl group as well as the nitrogen atom of the imine group coordinated with Al^{3+}. Furthermore, the proposed sensing mechanism of **HL** to Al^{3+} was illustrated in Scheme 2 according to the above results. In the absence of Al^{3+}, the nitrogen atom of imine could transfer an electron to the naphthalene ring (PET ON) and **HL** could transfer a hydroxyl proton to a neighboring imine nitrogen along with the formation of intramolecular hydrogen bond (OH ---- N) (ESIPT), which resulted in no fluorescence emission at 475 nm [44]. Upon addition of Al^{3+} to the system of **HL**, the oxygen atoms of hydroxyl group and the carbonyl group as well as the nitrogen atom of the imine group participated in the coordination of **HL** with Al^{3+}, which inhibited

ACCEPTED MANUSCRIPT

ACCEPTED MANUSCRIPT

the process of PET and ESIPT accompanied with remarkable fluorescence enhancement at 475 nm.

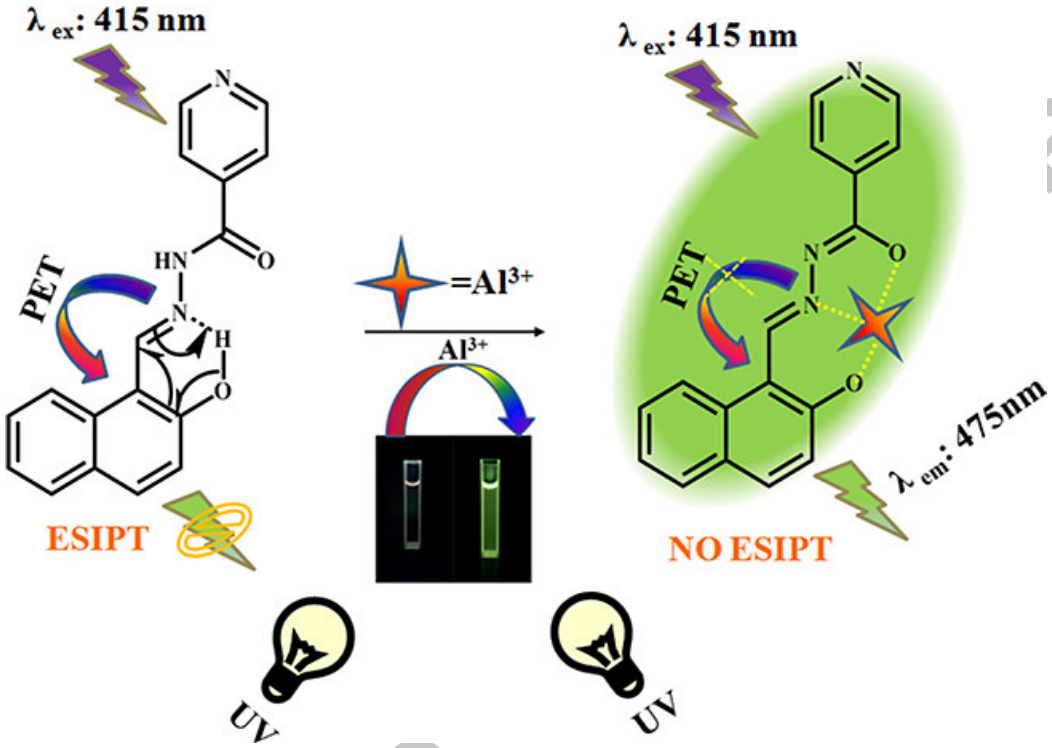

Scheme 2. The proposed sensing mechanism of **HL** with Al^{3+}.

4. Conclusion

In summary, we have designed and synthesized a simple naphthalene-based fluorescent probe **HL** which exhibited high selectivity for Al^{3+} in the aqueous solution. Compared with other fluorescent probes for Al^{3+} previously reported, **HL** showed a specific fluorogenic response towards Al^{3+} based on multi-mechanism (PET and ESIPT) in the fully aqueous solution, which enhanced potential practical application of **HL** for the detection of Al^{3+} in both biological assays and the environmental systems. What's more exciting, the sensing process of **HL** to Al^{3+} was chemically reversible by adding Na_2EDTA. The reversible phenomenon indicated that **HL** could be used circularly and repeatedly for the detection of Al^{3+}.

ACCEPTED MANUSCRIPT

Acknowledgments

This work is supported by the National Natural Science Foundation of China (81171337). Gansu NSF (1308RJZA115).

References

[1] (a) Silva, A. P.; Gunaratne, H. Q. N.; Gunnlaugsson, T.; Huxley, A. J. M.; McCoy, C. P.; Rademacher, J. T.; Rice, T. E. *Chem. Rev.* **1997**, 97, 1515; (b) Kim, H. N.; Ren, W. X.; Kim, J. S.; Yoon, J. *Chem. Soc. Rev.* **2012**, 41, 3210; (c) Goswami, S.; Manna, A.; Aich, K.; Paul, S. *Chem. Lett.* **2012**, 41, 1600; (d) Goswami, S.; Manna, A.; Maity, A. K.; Paul, S.; Das, A. K.; Das, M. K.; Saha, P.; Quah, C. K.; Fun, H. K. *Dalton Trans.* **2013**, 42, 12844.

[2] Tateno, K.; Ogawa, R.; Sakamoto, R.; Tsuchiya, M.; Otani, T.; Saito, T. *Org. Lett.* **2014**, 16, 3212.

[3] Outlaw, V. K.; Zhou, J. W.; Bragg, A. E.; Townsend, C. A. *RSC Adv.* **2016**, 6, 61249.

[4] Zhang, W. S.; Tang, B.; Liu, X.; Liu, Y. Y.; Xu, K. H.; Ma, J. P.; Tong, L. L.; Yang, G. W. *Analyst.* **2009**, 134, 367.

[5] Zhou, J. W.; Outlaw, V. K.; Townsend, C. A.; Bragg, A. E. *Chem. Eur. J.* **2016**, 22, 15212.

[6] Goswami, S.; Paul, S.; Manna, A. *RSC Adv.* **2013**, 3, 25079.

[7] Boonkitpatarakul, K.; Wang, J. F.; Niamnont, N.; Liu, B.; McDonald, L.; Pang, Y.; Sukwattanasinitt, M. *ACS Sens.* **2016**, 1, 144.

[8] Goswami, S.; Paul, S.; Manna, A. *RSC Adv.* **2013**, 3, 10639.

ACCEPTED MANUSCRIPT

[9] Maity, D.; Govindaraju, T. *Chem. Commun*. **2010**, 46, 4499.

[10] Sen, S.; Mukherjee, T.; Chattopadhyay, B.; Moirangthem, A.; Basu, A.; Marek, J. *Analyst*. **2012**, 137, 3975.

[11] Miller, W. S.; Zhuang, L.; Bottema, J.; Wittebrood, A. J.; Smet, P. D.; Haszler, A.; Viereggec, A. *Mater. Sci. Eng*. **2000**, 280, 37.

[12] Doherty, R. E. *Environ. Forensic.* **2000**, 1, 83.

[13] Ciardelli, G.; Ranieri, N. *Water Res.* **2001**, 35, 567.

[14] Robinson, G. H. *Chem. Eng. News.* **2003**, 81, 54.

[15] Scerri, E. R. *Oxford University Press.* **2007**.

[16] Exley, C. *Journal of Inorganic Biochemistry.* **2005**, 99, 1747.

[17] Gui, S.; Huang, Y.; Hu, F.; Jin, Y.; Zhang, G.; Yan, L.; Zhang, D.; Zhao, R. *Anal. Chem.* **2015**, 87, 1470.

[18] Guo, A. L.; Zhu, R. T.; Ren, Y. H.; Dong, J. L.; Feng, L. H. *Spectrochim. Acta, Part A*. **2016**, 153, 530.

[19] Maity, D.; Govindaraju, T. *Inorg. Chem.* **2010**, 49,7229.

[20] Sahana, A.; Banerjee, A.; Lohar, S.; Banik, A.; Mukhopadhyay, S. K.; Safin, D. A.; Babashkina, M. G.; Bolte, M.; Garcia, Y.; Das, D. *Dalton Trans.* **2013**, 42, 13311.

[21] Banerjee, A.; Sahana, A.; Das, S.; Lohar, S.; Sarkar, B.; Mukhopadhyay, S. K.; Mukherjee, A. K.; Das, D. *Analyst.* **2012**, 137, 2166.

[22] Jung, J. Y.; Han, S. J.; Chun, J.; Lee, C.; Yoon, J. *Dyes Pigm.* **2012**, 94, 423.

[23] Yun, S.; Kim, Y. O.; Kim, D.; Kim, H. G.; Ihm, H.; Kim, J. K.; Lee, C. W.; Lee, W. J.; Yoon, J.; Oh, K. S.; Yoon, J.; Park, S. M.; Kim, K. S. *Org. Lett.* **2003**, 5, 471.

ACCEPTED MANUSCRIPT

ACCEPTED MANUSCRIPT

[24] Goswami, S.; Manna, A.; Paul, S.; Aich, K.; Das, A. K.; Chakraborty, S. *Dalton Trans.* **2013**, 42, 8078.

[25] Liu, Z. D.; Xu, H. J.; Sheng, L. Q.; Chen, S. S.; Huang, D. Q.; Liu, J. *Spectrochim. Acta, Part A.* **2016**, 157, 6.

[26] Andrea, B. B.; Ana, C.; Salvador, M. G.; Margarita, P.; Juan, S.; Ramon, M. M.; Felix, S. *Chem. Commun.* **2012**, 48, 3000.

[27] Paul, S.; Goswami, S.; Manna, A. *Dalton Trans.* **2015**, 44, 11805.

[28] Anupam, G.; Jahangir, M.; Shubhamoy, C.; Goutam, P. *Dalton Trans.* **2016**, 45, 11540.

[29] Hwang, I. H.; Choi, Y. W.; Kim, K. B.; Park, G. J.; Lee, J. J.; Nguyen, L. T.; Noh, I.; Kim, C. *New J. Chem.* **2016**, 40, 171.

[30] Nandi, S.; Das, D. *ACS Sens.* **2016**, 1, 81.

[31] Chatterjee, N.; Maity, S. B.; Samadder, A.; Mukherjee, P.; Khuda-Bukhsh, A. R.; Bharadwaj, P. K. *RSC Adv.* **2016**, 6, 17995.

[32] Chen, X. J.; Shen, X. Y.; Guan, E. J.; Liu, Y.; Qin, A. J.; Sun, J. Z.; Tang, B. Z. *Chem. Commun.* **2013**, 49, 1503.

[33] Samanta, S.; Goswami, S.; Ramesh, A.; Das, G. *Sensor. Actuators B.* **2014**, 194, 120.

[34] Das, S.; Dutta, M.; Das, D. *Anal. Methods.* **2013**, 5, 6262.

[35] Liu, B.; Wang, P. F.; Chai, J.; Hu, X. Q.; Gao, T. T.; Chao, J. B.; Chen, T. G.; Yang, B. S. *Spectrochim. Acta, Part A.* **2016**, 168, 98.

[36] Kim, S.; Noh, Y.; Kim, K. Y.; Kim, J. H.; Kang, H. K.; Nam, S. W.; Kim, S. H.;

ACCEPTED MANUSCRIPT

ACCEPTED MANUSCRIPT

Park, S.; Kim, C.; Kim, J. *Inorg. Chem.* **2012**, 51, 3597.

[37] Ali, M.; Jha, M.; Das, S. K.; Saha, S. K. *J. Phys. Chem. B.* **2009**, 113, 15563.

[38] Goswami, S.; Manna, A.; Paul, S.; Maity, A. K.; Saha, P.; Quah, C. K.; Fun, H. K. *RSC Adv.* **2014**, 4, 34572.

[39] Qin, J. C.; Fan, L.; Li, T. R.; Yang, Z. Y. *Synth. Metals.* **2015**, 199, 179.

[40] Song, E. J.; Kim, H.; Hwang, I. H.; Kim, K. B.; Kim, A. R. *Sensor. Actuators B.* **2014**, 195, 36.

[41] Abebe, F. A.; Sinn, E. *Tetrahedron Lett.* **2011**, 52, 5234.

[42] Jang, Y. J.; Yeon, Y. H.; Yang, H. Y.; Noh, J. Y.; Hwang, I. H.; Kim, C. *Inorg. Chem. Commun.* **2013**, 33, 48.

[43] Yue, X. L.; Li, C. R.; Yang, Z. Y. *Inorg. Chim. Acta.* **2017**, 464, 167.

[44] Liu, Z. P.; He, W. J.; Guo, Z. J. *Chem. Soc. Rev.* **2013**, 42, 1568.

ACCEPTED MANUSCRIPT

ACCEPTED MANUSCRIPT

List of Figure captions

Figure 1. (a) UV-vis spectrum of **HL** before and after of *1 equiv. of* various metal cations in aqueous solution. (b) UV-vis absorption titration spectrum of **HL** (50 μM) with Al^{3+} (0-1.5 equiv.) in aqueous solution. Inset: Changes of absorbance intensity at 432 nm.

Figure 2. (a) The fluorescence emission spectrum of **HL** (50 μM) upon addition of *1 equiv. of* various metal ions (Na^{+}, K^{+}, Ag^{+}, Ca^{2+}, Mg^{2+}, Ba^{2+}, Zn^{2+}, Cu^{2+},Ni^{2+}, Cd^{2+}, Co^{2+}, Pb^{2+}, Mn^{2+}, Hg^{2+}, Cr^{3+}, Fe^{3+}, and Al^{3+}) in aqueous solution (λ_{ex}=415 nm; λ_{em}=475 nm). (b) The fluorescence emission spectrum of **HL** (50 μM) upon addition of Al^{3+} (0-1 equiv.) in aqueous solution (λ_{ex}=415 nm) Inset: Changes of fluorescence emission intensity at 475 nm.

Figure 3. The fluorescence intensity at 475 nm of **HL** (50 μM) upon addition of various metal ions (black bars: **HL** with other metal ions; red bars: **HL** with other metal ions and Al^{3+}) in aqueous solution (λ_{ex}=415 nm).

Figure 4. (a) The reversible experiment of **HL** towards Al^{3+} by adding Na_2EDTA in aqueous solution (λ_{ex}=415 nm). (b) The fluorogenic response of **HL** to Al^{3+} in the 5×10^{-3} M of Na_2EDTA over five complex/stripping cycles (λ_{ex}=415 nm).

Figure 5. Job's plot for determining the binding stoichiometry of **HL** and Al^{3+} in aqueous solution. The total concentration of **HL** and Al^{3+} was kept 100 μM (λ_{ex}=415 nm).

Figure 6. The ^{1}H NMR spectrum of **HL** with and without Al^{3+} in DMSO-d_6 (400

ACCEPTED MANUSCRIPT

MHz): **HL** (2); **HL** with *1 equiv of* Al^{3+} (1). Inset: The image of the structure of **HL**.

Scheme 1. The synthetic route of 2-hydroxy-1-naphthaldehyde-(4-pyridinecarboxylic) hydrazone (**HL**). Reagents and conditions: (a) HMTA, glacial acetic acid, reflux, 12 h; (b) EtOH, reflux, 10 h.

Scheme 2. The proposed sensing mechanism of **HL** with Al^{3+}.

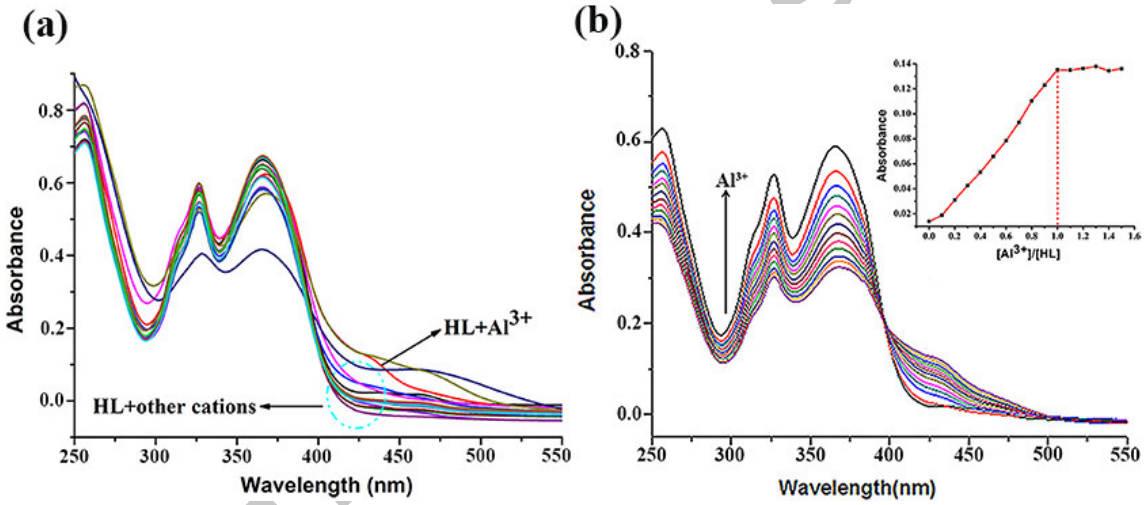

Figure 1. (a) UV-vis spectrum of **HL** before and after of *1 equiv. of* various metal cations in aqueous solution. (b) UV-vis absorption titration spectrum of **HL** (50 μM) with Al^{3+} (0-1.5 equiv.) in aqueous solution. Inset: Changes of absorbance intensity at 432 nm.

ACCEPTED MANUSCRIPT

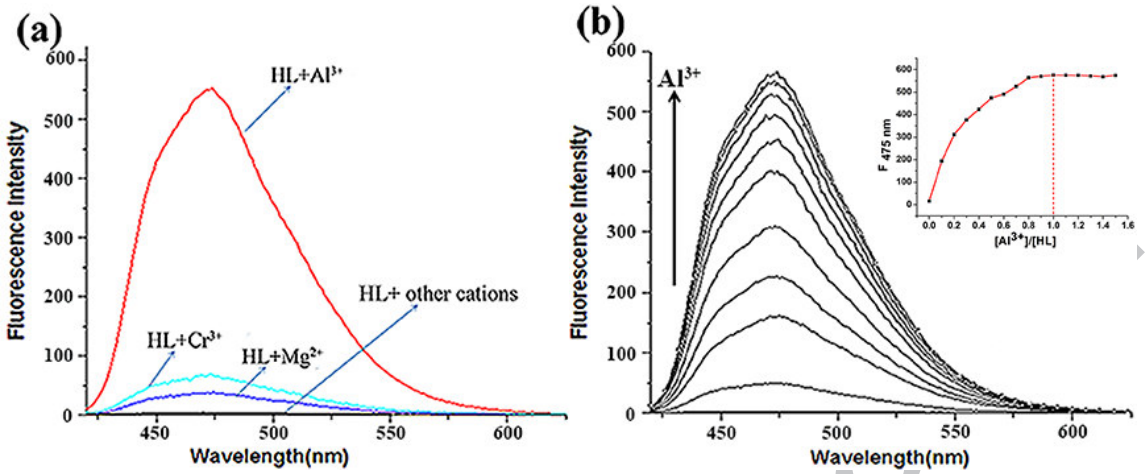

Figure 2. (a) The fluorescence emission spectrum of **HL** (50 μM) upon addition of *1 equiv. of* various metal ions (Na^{+}, K^{+}, Ag^{+}, Ca^{2+}, Mg^{2+}, Ba^{2+}, Zn^{2+}, Cu^{2+},Ni^{2+}, Cd^{2+}, Co^{2+}, Pb^{2+}, Mn^{2+}, Hg^{2+}, Cr^{3+}, Fe^{3+}, and Al^{3+}) in aqueous solution (λ_{ex}=415 nm; λ_{em}=475 nm). (b) The fluorescence emission spectrum of **HL** (50 μM) upon addition of Al^{3+} (0-1 equiv.) in aqueous solution (λ_{ex}=415 nm) Inset: Changes of fluorescence emission intensity at 475 nm.

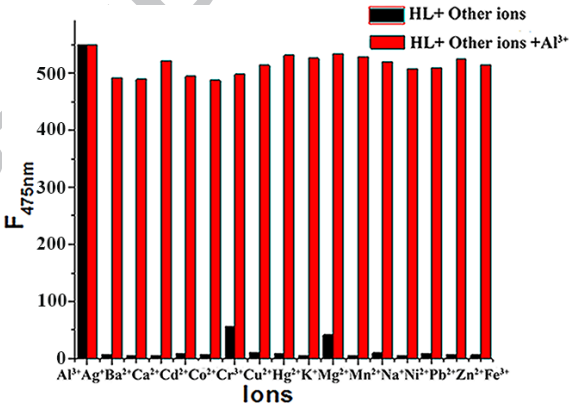

Figure 3. The fluorescence intensity at 475 nm of **HL** (50 μM) upon addition of various metal ions (black bars: **HL** with other metal ions; red bars: **HL** with other metal ions and Al^{3+}) in aqueous solution (λ_{ex}=415 nm).

ACCEPTED MANUSCRIPT

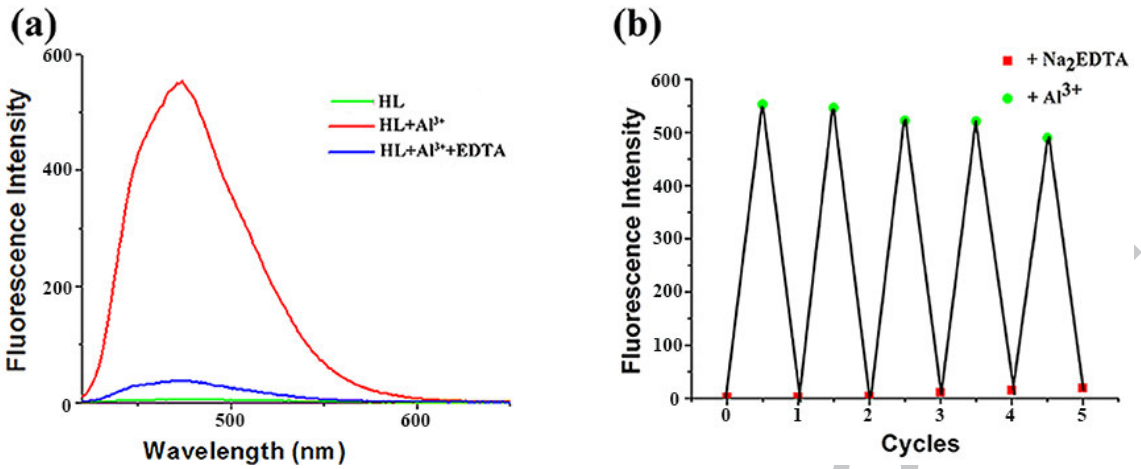

Figure 4. (a) The reversible experiment of **HL** towards Al^{3+} by adding Na_2EDTA in aqueous solution (λ_{ex}=415 nm). (b) The fluorogenic response of **HL** to Al^{3+} in the 5 × 10^{-3} M of Na_2EDTA over five complex/stripping cycles (λ_{ex}=415 nm).

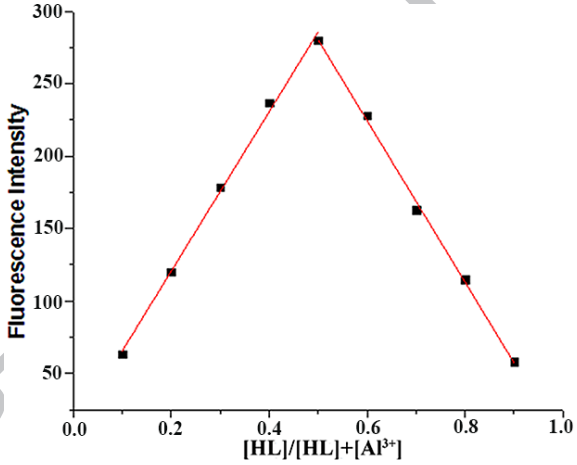

Figure 5. Job's plot for determining the binding stoichiometry of **HL** and Al^{3+} in aqueous solution. The total concentration of **HL** and Al^{3+} was kept 100 μM (λ_{ex}=415 nm).

ACCEPTED MANUSCRIPT

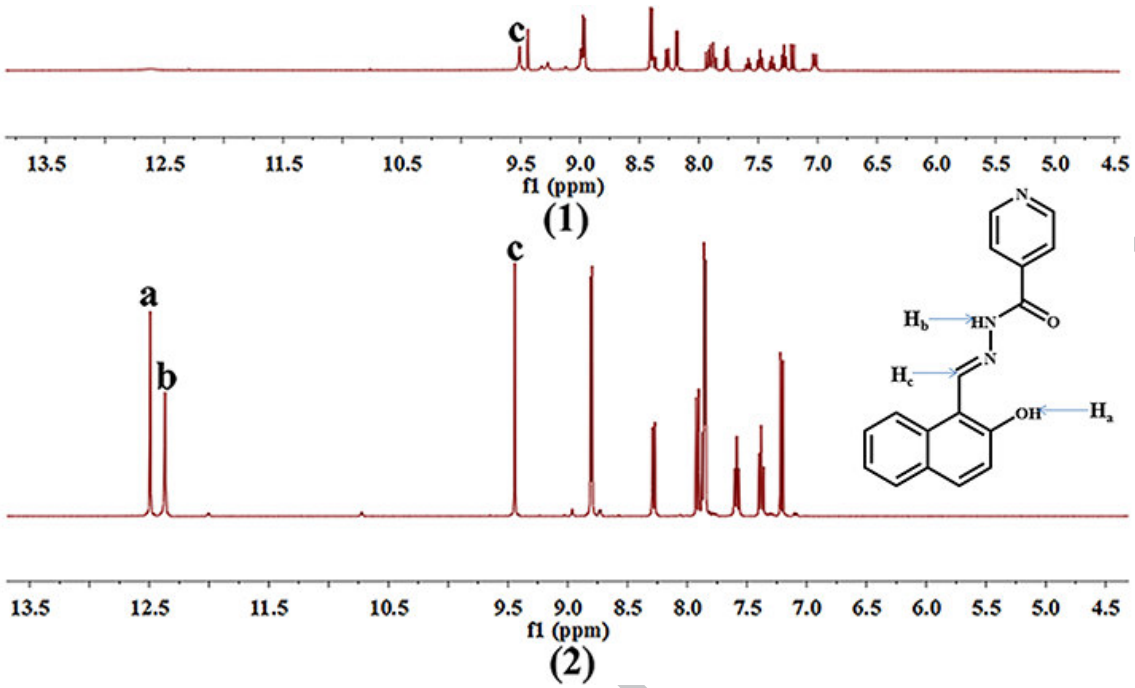

Figure 6. The ^{1}H NMR spectrum of **HL** with and without Al^{3+} in DMSO-d_6 (400 MHz): **HL** (2); **HL** with *1 equiv of* Al^{3+} (1). Inset: The image of the structure of **HL**.

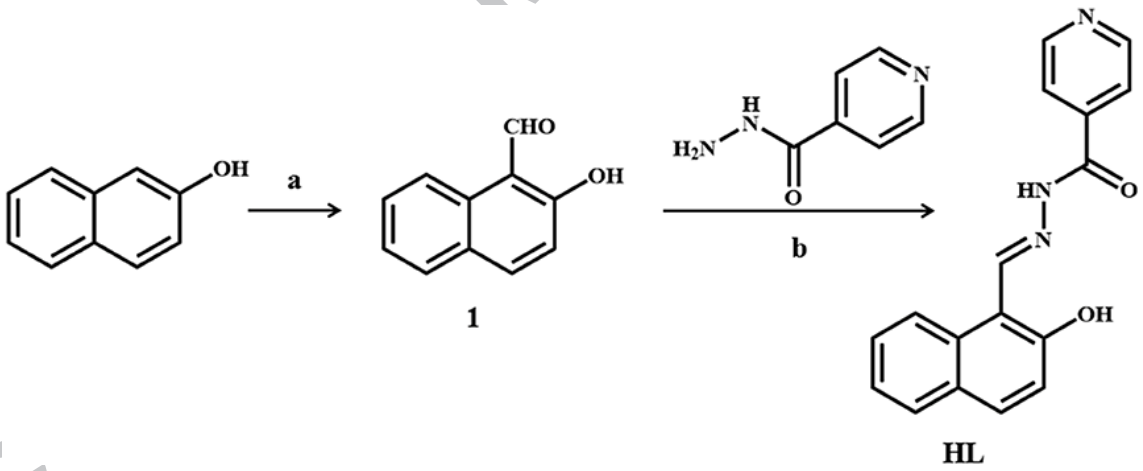

Scheme 1. The synthetic route of 2-hydroxy-1-naphthaldehyde-(4-pyridinecarboxylic) hydrazone (**HL**). Reagents and conditions: (a) HMTA, glacial acetic acid, reflux, 12 h; (b) EtOH, reflux, 10 h.

ACCEPTED MANUSCRIPT

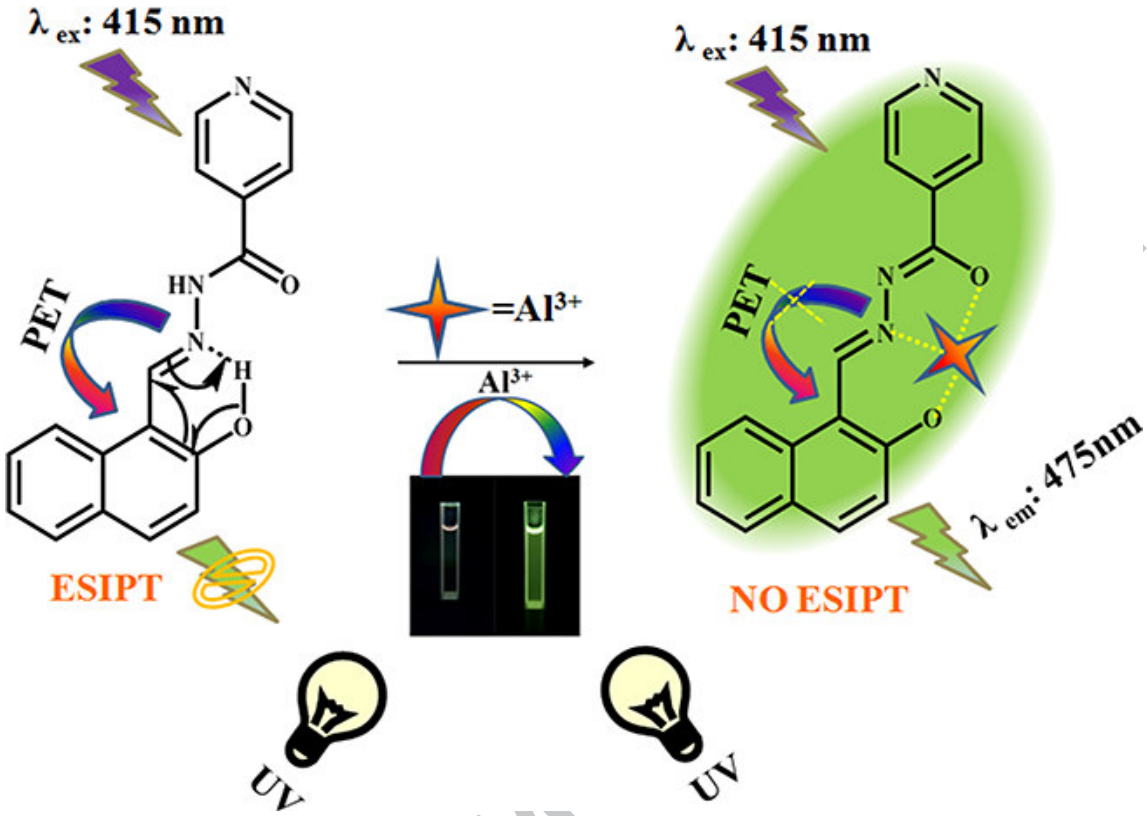

Scheme 2. The proposed sensing mechanism of **HL** with Al^{3+}.

ACCEPTED MANUSCRIPT

ACCEPTED MANUSCRIPT

Graphical abstract

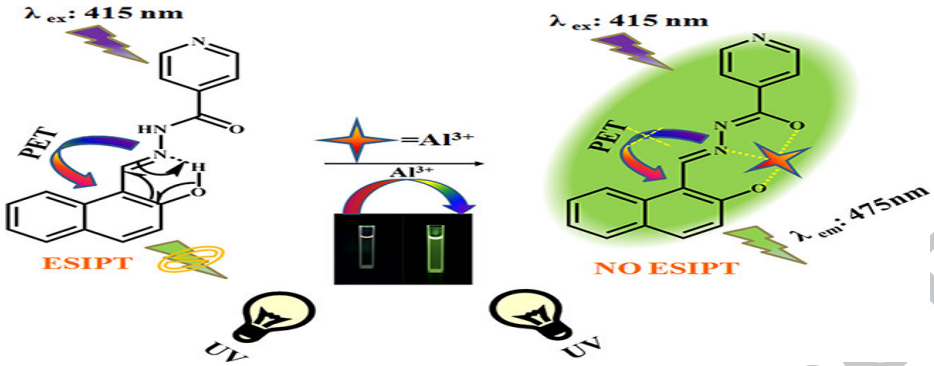

ACCEPTED MANUSCRIPT

ACCEPTED MANUSCRIPT

Highlights

- A simple naphthalene-derived Al^{3+}-selective fluorescent chemosensor was designed and synthesized.
- The binding stoichiometry between **HL** and Al^{3+} was determined to be 1 :1 by the Job's plot and ESI-MS spectrum data.
- The recognition process of **HL** towards Al^{3+} was chemically reversible by adding Na_2EDTA.
- **HL** exhibited a specific fluorogenic response towards Al^{3+} based on multi-mechanism (PET and ESIPT) in fully aqueous solution.
- The proposed sensing mechanism was investigated by the ^1H NMR titration experiment in detail.

ACCEPTED MANUSCRIPT